

University of Louisville

## ThinkIR: The University of Louisville's Institutional Repository

---

Electronic Theses and Dissertations

---

8-2019

### Non-viral transfection efficiencies for the advancement of CAR-T therapy.

Emily M Murphy  
*University of Louisville*

Follow this and additional works at: <https://ir.library.louisville.edu/etd>



Part of the [Therapeutics Commons](#)

---

#### Recommended Citation

Murphy, Emily M, "Non-viral transfection efficiencies for the advancement of CAR-T therapy." (2019). *Electronic Theses and Dissertations*. Paper 3248.  
<https://doi.org/10.18297/etd/3248>

This Master's Thesis is brought to you for free and open access by ThinkIR: The University of Louisville's Institutional Repository. It has been accepted for inclusion in Electronic Theses and Dissertations by an authorized administrator of ThinkIR: The University of Louisville's Institutional Repository. This title appears here courtesy of the author, who has retained all other copyrights. For more information, please contact [thinkir@louisville.edu](mailto:thinkir@louisville.edu).

NON-VIRAL TRANSFECTION EFFICIENCIES FOR THE ADVANCEMENT OF  
CAR-T THERAPY

By

Emily Margaret Murphy  
B.S. Bioengineering, University of Louisville, May 2018

A Thesis  
Submitted to the Faculty of the  
University of Louisville  
J.B. Speed School of Engineering  
as Partial Fulfillment of the Requirements  
for the Professional Degree

MASTER OF ENGINEERING

Department of Bioengineering

August 2019



NON-VIRAL TRANSFECTION EFFICIENCIES FOR THE ADVANCEMENT OF  
CAR-T THERAPY

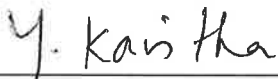
Submitted by:   
Emily M. Murphy

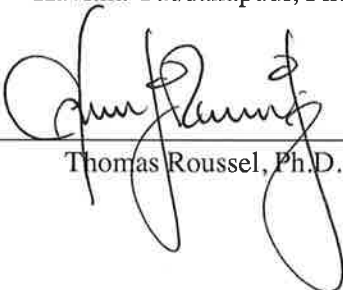
A Thesis Approved On

July 31, 2019  
(Date)

By the Following Reading and Examination Committee:

  
Jonathan A. Kopechek, Thesis Director

  
Kavitha Yaddanapudi, Ph.D.

  
Thomas Roussel, Ph.D.

## ACKNOWLEDGEMENTS

First and foremost, I would like to thank my committee members for this guidance and support on this project in addition to taking time out of their busy schedules to read and revise my thesis and be present at my oral defense.

Dr. Jonathan Kopechek

Dr. Kavitha Yaddanapudi

Dr. Thomas Roussel

I would like to thank everyone in both Dr. Jonathan Kopechek's lab and Dr. Kavitha Yaddanapudi's lab for their help, guidance, support, and kindness towards me.

Mariah Priddy

Gavin Poff

Connor Centner

Bryce Stamp

Daniel Hodge

Dr. Justin Farge

Meghan Otto

Bryce Stamp, cheers to all of the T-cells we isolated and long mornings we talked about life. I thank you for working closely with me on every T-cell experiment that built this thesis; troubleshooting, brainstorming, and thinking through what to do better in the future. I wish you the best of luck in your future medical school career! You will make a great doctor.

Dr. Kopechek, where do I even begin? Thank you for taking a chance on me as a co-op student. Thank you for being patient as I learned the very beginning skills as a researcher and teaching me to be a better writer and presenter. Thank you for pushing to me do my best and grow

in all areas of lab work. Thank you for funding my research trips and allowing me to adventure in Phoenix, Washington DC, Atlanta, and soon zero gravity. You have been the best boss, mentor, father figure, and friend. I wish you and your family the best in the upcoming years and I hope to see you soon.

Lastly, I would like to thank my family, friends, and boyfriend. Not only have they believed in me since the beginning but continuously express their love and support in times of need. I would not have made it this far without them.

From those who I worked with before this master's project began, to those I will end this journey with, you have all helped mold me into the researcher, student, friend, and daughter I am today.

## ABSTRACT

Leukemias are the most common form of childhood cancer making up 30% of total pediatric oncological cases, and Acute Lymphoblastic Leukemia (ALL) makes up a significant portion (12%) of the total pediatric cancer diagnoses. In 2017, the FDA approved a successful immunotherapy called CAR-T therapy for the treatment of pediatric B-cell ALL. This therapy includes a CAR (chimeric antigen receptor) that is loaded into the T-cell and expressed. Currently, the loading of the CAR utilizes viral transduction, but consistency issues lead to adverse symptoms in the patients. Better methods of transduction/transfection are being studied in order to improve these consistency concerns. In this thesis, the efficiency of sonoporation as a non-viral method of transfection was assessed. Fluorescein was loaded as a fluorescent model molecule for beginning understanding of the sonoporation efficiency. It was found that by using sonoporation over electroporation for the uptake of fluorescein, the efficiency is improved by 34%. When sonoporation was used for the transfection of GFP plasmid, the same increase was not proven. This leads to the conclusion that without further optimization, sonoporation is successful at loading small molecule such as fluorescein but not those as large as plasmids. With optimization, sonoporation could eventually be used as a non-viral method to transfect T-cells with CARs for CAR-T therapy and the treatment of ALL in both children and adults.

## TABLE OF CONTENTS

	<u>Page</u>
APPROVAL PAGE.....	ii
ACKNOWLEDGMENTS.....	iii
ABSTRACT.....	v
LIST OF TABLES.....	vii
LIST OF FIGURES.....	viii
I. INTRODUCTION.....	1
Objective .....	1
Overview of Acute Lymphoblastic Leukemia.....	1
Pathobiology .....	2
Symptoms .....	4
Diagnosis.....	5
Treatment (leading up to CAR-T) .....	6
CAR-T Therapy, an Engineering Solution.....	8
Transfection Overview.....	9
Viral Transduction.....	11
Electroporation.....	12
Cationic Transfection Reagents.....	13
Sonoporation/Ultrasound-mediated Delivery .....	13
Ultrasonic Flow System .....	14
CAR-T Shortcomings and Room for Improvement .....	16
II. PROCEDURE.....	18
Fabrication/Setup of Device .....	18
A549 Cell Culture and Harvesting.....	18
Primary T-Cell Isolation .....	19
Microbubble Synthesis.....	19
Bacteria Growth and GFP Plasmid Isolation .....	20
Lipofectamine-3000 Experiments.....	21
Electroporation .....	21
Sonoporation .....	22
Flow Cytometry Analysis.....	22
Statistical Analysis.....	23
III. RESULTS/DISCUSSION.....	24
Fluorescein Loading Studies.....	24
GFP Plasmid Transfection Studies .....	30
Microscopy Analysis .....	38
IV. CONCLUSION.....	39
V. RECOMMENDATIONS.....	40
REFERENCES.....	41
VITA.....	45



## LIST OF TABLES

	<u>Page</u>
TABLE 1: TRANSFECTION METHODS .....	10

## LIST OF FIGURES

	<u>Page</u>
Figure 1: ALL Gene Translocation .....	2
Figure 2: Blood Smears .....	5
Figure 3: Sonoporation.....	14
Figure 4: Ultrasonic Flow Device and Microfluidics Channel Design .....	15
Figure 5: Microscopy Image of Microfluidics Device .....	16
Figure 6: Primary T-Cells Microbubble Dose Study Histogram.....	24
Figure 7: Primary T-Cells Microbubble Dose Study Bar Graph.....	25
Figure 8: Red Blood Cell Microbubble Dose Study Bar Graph .....	26
Figure 9: Primary T-Cell Fluorescein Transfection Study Histogram .....	26
Figure 10: Primary T-Cell Sonoporation Histogram .....	27
Figure 11: Primary T-Cell Fluorescein Transfection Study Bar Graph .....	28
Figure 12: Primary T-Cells vs. Jurkat. Cells Electroporation Study Histogram .....	29
Figure 13: Primary T-Cells vs. Jurkat. Cells Electroporation Study Bar Graph.....	30
Figure 14: Primary T-Cell Sonoporation Microbubble Composition Study Histogram .....	31
Figure 15: Primary T-Cell Sonoporation Microbubble Composition Study Bar Graph .....	31
Figure 16: Primary T-Cell Sonoporation Timepoint Histograms.....	32
Figure 17: Primary T-Cell Sonoporation Timepoint Histograms cont.....	33
Figure 18: Primary T-Cell Sonoporation Timepoint Bar Graph.....	33
Figure 19: Sonoporation Transfection of A549 Cells .....	34
Figure 20: Lipofectamine Transfection of Primary T-Cells and A549 Cells .....	35
Figure 21: Electroporation Transfection of Primary T-Cells and A549 Cells .....	36
Figure 22: Microscopy Imaging of Electroporation Transfection.....	38
Figure 23: Microscopy Imaging of Lipofectamine Transfection .....	38

## I. INTRODUCTION

### *Objective*

The objective of this thesis is to assess the efficiency of sonoporation to transfect primary T-cells with plasmid for its potential use as a non-viral method of transfection for CAR-T therapy for patients battling Acute Lymphoblastic Leukemia.

### *Overview of Acute Lymphoblastic Leukemia*

Acute Lymphoblastic Leukemia (ALL) is a malignant bone marrow disease where early lymphoid precursors proliferate and replace normal cells. It can arise from several genetic mutations in either B- or T-progenitor cells that result in the overproduction of these immune cells. If mistreated or left untreated, the genetic mutation can lead to a lethal buildup of leukemic cells in the body [1, 2].

Leukemias are the most common form of childhood cancer making up 30% of total pediatric oncological cases, and ALL makes up a significant portion (12%) of the total pediatric cancer diagnoses. Its population distribution is bimodal, however, with one population centered around age 4-5 and another age 50+. Children 5 years and younger are at the highest risk of developing this disease and this thesis focuses mainly on pediatric ALL [3]. Fortunately, the patient response to current treatments has allowed for an 98% remission rate in children and an 85% five-year survival rate where patients are considered cancer-free.

The steps of hemopoiesis begins with a blood stem cell, referred to as a hemopoietic stem cell. This stem cell differentiates into either a myeloid stem cell or a lymphoid stem cell. On the myeloid side, the stem cell further differentiates into red blood cells, platelets, or a myeloblast. The differentiation then terminates after myeloblasts develop into granulocytes (eosinophils, basophils, or neutrophils). Going back to the lymphoid stem cell line, these stem cells differentiate into lymphoblasts first, followed by B lymphocytes, T lymphocytes, or Natural Killer (NK) cells. The three granulocytes in addition to the lymphoblasts make up what is considered white blood cells which are vital cells in the immune system and this is where the problems originate in ALL [4]. Many sub-classifications of ALL exist, however only three differ therapeutically: B-cell precursor, T-Cell precursor, and mature B-Cell [1, 2]. Knowing the cell lineage is important as proper diagnosis is crucial for an oncologist to determine an effective treatment regimen.

### *Pathobiology*

Although it is rare for an adult to develop ALL, B-cell precursor ALL is the most common type of the adult form of the disease [1, 2]. The TEL-AML1 fusion gene is the distinguishing mutation in B-cell precursor ALL. This gene is generated by the

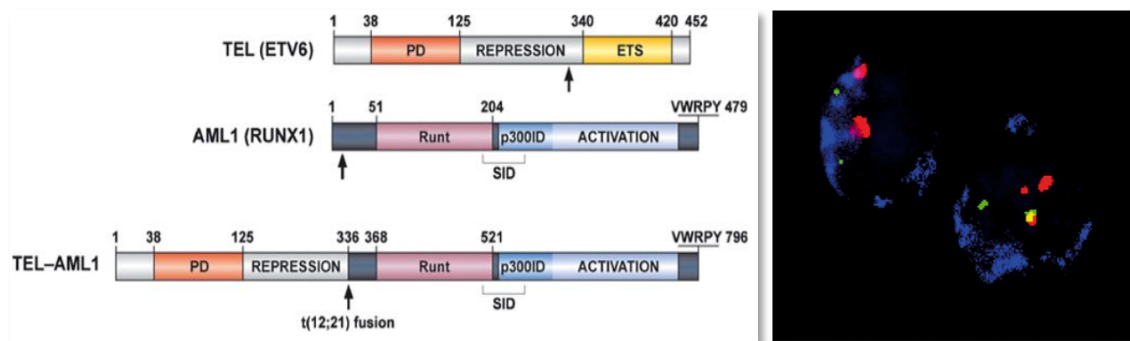


Figure 1A (left): A schematic representation of the translocation process during the TEL-AML1 fusion. This translocation occurs between chromosome 12 and 21 [5].  
 Figure 1B (right): Microscopic representation of the TEL-AML1 gene fusion. Red = AML1 gene, Green = TEL gene, Blue = CD10 (leukemic antibody), Yellow = colocalization of the genes [5].

t(12;21)(p13;q22) chromosomal translocation (Figure 1) [5]. The TEL gene is significant in the natural development of hematopoietic cells during hemopoiesis. The AML1 gene is significant in embryonic hemopoiesis. The fusion of these two genes creates problems in the development of B-lineage lymphocytes [5].

Another type of ALL is T-cell precursor which can be defined in 50% of its cases by mutations involving the NOTCH1 gene. This gene mutation is generated by the t(7;9)(q34;q34.3) translocation. NOTCH regulates normal T-cell development through the creation of a transmembrane receptor. The mutation causes an overexpression of an active form of NOTCH that inhibits cell differentiation [6].

In 20-30% of ALL cases occurs what is called the Philadelphia chromosome, or the t(9;22) chromosomal translocation, meaning a fragment of chromosome 9 switches places with a fragment of chromosome 22. In these cases, the B-cell antigen receptor (BCR) signaling protein binds to the Abelson (ABL) non-receptor tyrosine kinase. This takes place on chromosome 22 where the broken off piece of chromosome 9 has attached. This results in tyrosine kinase activity overdrive and the interaction of this fused protein with other elements such as the signaling protein for RAS (renin-angiotensin system). Fortunately, it has been discovered that Imatinib Mesylate, a chemotherapeutic drug, selectively targets this gene fusion and has proven effective in Philadelphia chromosome-specific cases. Imatinib mesylate works by inhibiting tyrosine kinase activity by binding to an intracellular pocket in the tyrosine kinase. This binding inhibits ATP binding and prevents phosphorylation that allows for cell growth [1, 2, 7, 8].

## *Symptoms*

The symptom list of ALL is broad, however it can be broken down into smaller categories to help discuss the multitude of symptoms. Symptoms caused by low numbers of blood cells in the patient can include fatigue, weakness, dizziness or lightheadedness, shortness of breath, pale skin, infections that are difficult to get rid of, bruising, and abnormal bleeding such as reoccurring nose bleeds or bleeding gums. The overcrowding of leukemic cells in the bone marrow make it difficult for the marrow to produce sufficient amounts of other blood cell types, such as red blood cells. Red blood cells are responsible for the delivery of oxygen to tissues in the body; therefore, a lack of red blood cells can cause anemia-like symptoms such as fatigue, weakness, dizziness and shortness of breath [4, 9, 10].

General symptoms that are harder to link to ALL include weight loss, fever, night sweats, and loss of appetite. These symptoms are considered non-specific and are most likely caused by something other than leukemia in the patient. However, these symptoms are indicative of the immune system working to rid the body of something unnatural. Abnormal or excess T-cells in the body stimulates the immune system, which is why these occurrences can be considered non-specific symptoms of ALL.

Symptoms caused by a buildup of cells include swelling in the abdomen, enlarged lymph nodes, bone or joint pain, and an enlarged thymus. Leukemia cells can build up in the liver or spleen, causing swelling and fullness in the abdomen of the patient. Feeling full after ingesting a small amount of food can indicate this swelling due to decreased room for expansion by the stomach. The pressure of the liver and spleen on other abdominal organs would also cause this sensation. Even though these organs are covered by the lower ribs, a

swollen liver and spleen are detectable by a palpation exam. If ALL spreads to the lymph nodes, the buildup of excess cells can cause swelling. This may be more obvious in the neck, groin, or underarm areas, however swelling of lymph nodes in the chest and abdomen can also occur. CT or MRI scans would be necessary to determine swelling in these areas. If there is a buildup of cells around bones or inside the joint, pain can also occur in these areas [4, 9, 10].

### *Diagnosis*

If symptoms discussed above occur in a patient, an oncologist will initiate what will become a lengthy diagnosis process. Blood tests, bone marrow biopsy and aspiration, lumbar puncture, immunophenotyping/genotyping all might be necessary in order to diagnose ALL [2]. During a blood smear, the oncologist will look for increased levels of lymphoblasts and lymphocytes which is proof of the overproduction of immune cells that

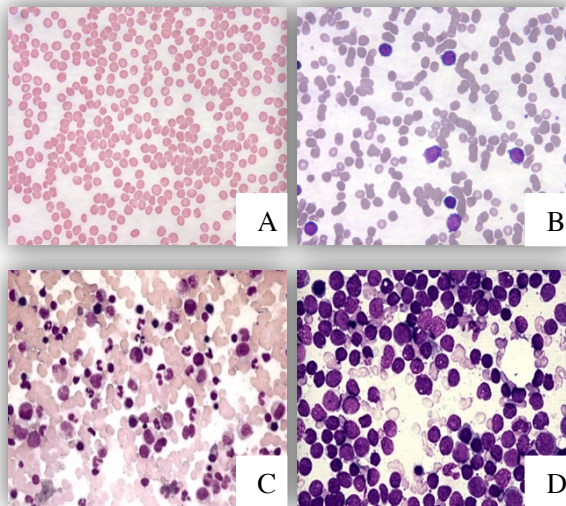


*Figure 2: Blood smears (images A and B) and bone marrow aspiration smears (images C and D) are a normal part of the diagnosis process for ALL. In diseased states, an increase in lymphoblasts and lymphocytes will be present in the blood and bone marrow (images B and D). These immune cells are dyed purple in the above microscopy [11].*

defines ALL [11] (Figure 2). A CBC (complete blood count) and differential blood count will also be conducted to evaluate the ratio of white blood cells in the blood. Elevated levels of lymphoblasts will also be measured in the bone marrow through bone marrow aspiration. A large needle will be inserted into either the hip bone or breast bone of the patient and bone marrow will be removed for evaluation. This process normally includes a bone/bone marrow biopsy simultaneous to the aspiration. In some cases, the leukemia will spread to the central nervous system and a lumbar puncture is required. Furthermore, immunophenotyping and genotyping is conducted to get a thorough diagnosis. Flow cytometry, RT-PCR, and fluorescent in-situ hybridization (FISH) are all utilized for this process. Flow cytometry can detect the presence of leukemic antibodies on the T-cells while RT-PCR and FISH can detect changes in the DNA and genetic makeup [2].

#### *Treatment (leading up to CAR-T)*

As discussed previously, the current treatments for ALL tend to be successful with a child remission rate of 98% and child five-year survival rate of 85% [1-3]. Current treatment methods include chemotherapy in three stages based on the patients' risk assessment and an allogeneic hemopoietic stem cell transplantation if necessary. In patients that express the Philadelphia Chromosome, tyrosine kinase inhibitors are instilled in addition to the chemotherapeutics.

The first stage of chemotherapy is called the remission-induction phase. Its goal is to eradicate 99% of the leukemic cells present in these patients and reinstate normal hemopoiesis. This stage commonly includes a three-drug cocktail consisting of a glucocorticoid (prednisone or dexamethasone), vincristine, and asparaginase or



anthracycline. This three-drug combination is usually sufficient for patients that are considered standard-risk. In high- to very high-risk patients, asparagine and anthracycline can both be administered, resulting in a four or more drug treatment [1, 2].

Following the remission-induction phase is the consolidation, or intensification, treatment phase. Once the patient shows signs of normal hemopoiesis the intensification process is meant to eliminate the drug-resistant leukemic cells. This elimination reduces the risk of relapse. Although currently there is not a consensus on the best treatment regimen, oncologists will often use high doses of methotrexate, mercaptopurine, frequent vincristine and corticosteroid dosages and high-dose asparaginase for 20-30 weeks. Reinduction treatment of the same drugs used during the induction-remission stages for the patient are often used during the intensification stages as well to further enhance treatment outcome. One study conducted in Philadelphia concluded that double reinduction treatment was vital to patient success while additional administration of vincristine and prednisone after one reinduction round was not useful [1, 2, 12].

Allogenic hemopoiesis stem-cell transplantation is conducted in patients when necessary. It is the most rigorous form of treatment for ALL and only utilized when necessary. The benefit in patients with high-risk ALL, Philadelphia Chromosome-positive patients, and adults with the t(4;11) translocation gene mutation has been proven, however the necessity in infant regimens is controversial. Finding a stem-cell match for patients can be difficult, as 7/10 patients do not have a human leukocyte antigen (HLA) match in their family and must rely on outside donors. Finding matches has become more common since the 1990s with the establishment of bone marrow registries such as Be the Match [13].

Continuation treatment takes place in most patients following their previous chemotherapy and possible stem cell transplantations. Although 2/3 of patients can be successfully treated within the first 12 months of treatment, often oncologists will continue their treatment for 2-2.5 years to decrease the chance of relapse. This continuation treatment includes daily mercaptopurine and methotrexate, often in pill or liquid form to be taken orally. Side effects of these medications include liver damage, high blood pressure, hair loss, and swelling of the body [14]. As with most treatment regimens, there are areas that still need to be improved. As our medical world advances, individualized treatments that utilize immunoengineering has become more common [1, 2].

#### *CAR-T Therapy, an Engineering Solution*

The earliest attempt at engineering T-cells for the treatment of ALL included expression of cloned T-cell receptors (TCR). These receptors can recognize intracellular and extracellular antigens in the context of the major histocompatibility complex (MHC) which is the all-encompassing term used for the surface proteins essential for the immune system to recognize and destroy foreign particles. The problem with this method is that many tumors downregulate MHC expression, making the detection by TCRs difficult. In 2017, the FDA approved a successful immunotherapy called CAR-T therapy for the treatment of pediatric B-cell ALL. In this therapy, an artificial receptor called a CAR (chimeric antigen receptor) is loaded into a patient's T-cells [15]. The expression of the CAR allows for detection of leukemic cells that express specific CD (cluster of differentiation) markers. The idea of CAR loading was first described in 1990 as a way to add specificity to tumor targeting methods. It was not until 2010, however, that the first

clinical trial took place [16, 17]. The CAR method of T-cell engineering is MHC-independent and has proven more successful than the TCR attempt [18].

The ideal antigen to target on cancer cells would be on the surface and a result of gene translocation or mutations occurring in these cells. This type of antigen is difficult to find, so the next best thing is CD19, the most common and successfully targeted antigen [19]. This is the antigen targeted in the FDA-approved treatment, tisagenlecleucel [8]. CD19 is expressed on the surface of B-cells and have a single cell lineage. Its function is replaceable, making it an ideal target for CAR-T treatment. It is not only expressed in ALL, but also chronic lymphocytic leukemia (CLL) and non-Hodgkin's lymphomas, meaning CAR-T targeting CD19 could treat multiple cancers types [16, 17].

One of the areas for improvement in current CAR-T therapy is the inconsistency of CAR-loading. Viral transduction causes random insertion into the genome. Variability in insertion can cause inconsistent levels of receptor expression. This is thought to be the cause for some adverse symptoms including cytokine release syndrome and neurotoxicity, in addition to high fever, delirium, seizures, and even coma in rare yet severe cases [20, 21]. One trigger of cytokine release syndrome is tumor lysis syndrome. If T-cells are overactive, too many cancer cells are killed at once. This causes an increased release of potassium, phosphorus, and nucleic acids from the cancer cells which can cause hyperuricemia, hyperkalemia, hyperphosphatemia, and hypocalcemia, and their related side effects [22]. In some retroviral reports, this random insertion approach has resulted in the creation of an oncogene [16, 17]. Guided gene editing, such as CRISPR-Cas9, or a change in the transfection/transduction method could potentially add consistency to the CAR expression.

### *Transfection Overview*

Artificial gene delivery into cells, a technique referred to as *transfection*, has become a large focus for the treatment of diseases. Cancer, heart failure, and hemophilia are just a few of the areas where transfection has proven significant for the discovery of new treatments. For many years viral transfection, a technique referred to as *transduction*, has been the primary technique for gene delivery. As problems with this method arose (such as safety and limitations in targeting and plasmid size) the search for non-viral methods began to take place. It was soon understood that non-viral methods have similar, if not better, success with penetrating the cell membrane. The areas in which improvements still exist for non-viral methods are the transfection efficiency, unwanted degradation of DNA, and limitations with nucleus translocation [23]. In this section we will explore the different forms of transfection along with the benefits and drawbacks of each (Table 1).

<b>Transfection Technique</b>	<b>Pros</b>	<b>Cons</b>
Viral Transfection (Transduction)	<ul style="list-style-type: none"> <li>• Inherent ability to transfect DNA</li> <li>• High transfection efficiency</li> <li>• Ability to translocate to the nucleus</li> </ul>	<ul style="list-style-type: none"> <li>• Gene randomly inserted</li> <li>• Safety – insertion mutagenesis</li> <li>• Manufacturing difficulties</li> <li>• Limitations of plasmid size</li> <li>• Limitations of targeting</li> </ul>
Electroporation	<ul style="list-style-type: none"> <li>• Pores stay open for minutes</li> <li>• Low toxicity</li> <li>• Low immunogenicity</li> <li>• Ease of manufacturing</li> </ul>	<ul style="list-style-type: none"> <li>• Microscale setups – throughput</li> <li>• Macroscale setups – transfection efficiency</li> <li>• Passive process</li> </ul>

		<ul style="list-style-type: none"> <li>• Optimization for different cell types (voltage, capacitance, temperature, etc.)</li> <li>• Lower transfection efficiency than viral methods</li> <li>• Pores stay open for minutes</li> </ul>
Cationic Transfection Reagents	<ul style="list-style-type: none"> <li>• Low toxicity</li> <li>• Low immunogenicity</li> <li>• Ease of manufacturing</li> </ul>	<ul style="list-style-type: none"> <li>• Lower transfection efficiency than viral methods</li> </ul>
Sonoporation	<ul style="list-style-type: none"> <li>• Active process – microjetting/microstreaming</li> <li>• Possible at low temperatures (4C), increasing cell viability</li> <li>• Spatiotemporal control</li> <li>• Noninvasive</li> <li>• Delivers to cytoplasm (in comparison to endosomal entrapment by other lipid based/nanoparticle endocytosis methods)</li> <li>• Low toxicity</li> <li>• Low immunogenicity</li> <li>• Ease of manufacturing</li> </ul>	<ul style="list-style-type: none"> <li>• Microscale setups – throughput</li> <li>• Lower transfection efficiency than viral method</li> <li>• Optimization necessary (bubble dose, flow rate, ultrasound settings, etc.)</li> </ul>

Table 1: A summary of the pros and cons of transfection methods.

### *Viral Transduction*

Transduction is the primary method used in gene therapy and CAR-T specifically (i.e. using viruses (viral vectors) to deliver DNA to a cell for gene insertion/modification.) The virus that is used as a vehicle for insertion does not contain enough of its DNA to replicate and is termed “replication-deficient.” Despite the fact that these viruses cannot replicate, transduction is not free of problems as safety is a major concern with viral transduction. Controlling the final destination of the sequence transferred by the virus is still difficult and can lead to insertional mutagenesis [23, 24]. Until sufficient assays arise

to predict these mutations, this problem surrounding random insertion will continue to exist. As more clinical trials are approved using these techniques, appropriate assays will become more necessary [24].

### *Electroporation*

In electrical terms, a cell membrane can be compared to a capacitor - storing electrical energy but not passing current without the assistance of ion channels. Considering this concept, one method of non-viral transfection is by administering electrical pulses to the membrane which allows for a temporary membrane breakdown; a process termed electroporation. Pores that can last a couple minutes are formed in the cell membrane which allows molecules such as nucleic acids to pass through via diffusion and potentially reach the nucleus [25, 26]. This technique has proven successful for both stable and transient transfection on many different cell types. However, optimizing the pulse duration, voltage intensity, and electroporation buffer being used is crucial for each cell type. Both high voltage with low capacitance (short pulse duration) and low voltage with high capacitance (long pulse duration) have transfected cell lines but the optimal parameters are different for each cell type. For example, primary cells are more sensitive and experience toxicity under high voltage, so short pulse durations would not be safe for the transfection of these cells. The optimal temperature at which the cells are electroporated can also vary, as keeping the cells on ice can improve viability but some long pulse duration treatments are most effective at room temperature. Commercial electroporation products have been made available, with programmable pulse duration and voltage to help ease the optimization process of different cell lines. This helped make electroporation a popular

non-viral technique for loading desired molecules into cells [26]. Challenges surrounding this technique remain - specifically how quickly large amounts of cells can be processed. In macro-scale setups, both transfection efficiency and cell viability may suffer. Meanwhile in micro-scale experimental setups, throughput and processing time for large cell amounts becomes a problem. When transfection is necessary, large amounts of cells are needed for the treatment to work effectively [27].

### *Cationic Transfection Reagents*

Another form of transfection involves cationic liposomes, polymers, proteins or peptides to permeate the cell membrane. Companies have released commercialized products to aid this technique, such as Lipofectamine by Thermo Fisher Scientific and Eugene by Promega. The cationic vehicles loaded with plasmid bind to surface proteins and activate signaling pathways that cue for endocytosis [23]. This form of non-viral transfection has not been shown to have higher transfection efficiency than viral methods, however it is less toxic and induces fewer immune responses.

### *Sonoporation/Ultrasound-mediated Delivery*

The process of exposing tissue to ultrasound waves to increase the permeability of the cell membrane is another form of non-viral transfection called sonoporation [28]. This process can be improved by the addition of lipid-shelled, gas-cored microbubbles. When the exposure to ultrasound pulses causes the microbubbles to oscillate, at sufficiently high amplitudes they can collapse (inertial cavitation) and create temporary pores in the cell membrane in addition to a microjet that can force the nearby liquid into the cells [29, 30].

In this way, sonoporation can be both an active and passive process in comparison to electroporation which relies more so on passive diffusion [29]. These transient pores can reseal as quickly as a minute after their creation, allowing the cell to swiftly recover and return to normal function. This process allows for spatiotemporal control, allowing for a vast array of possible therapeutic uses, including mammalian cell transfection [31].

### *Ultrasonic Flow System*

One proposed method to add consistency to the loading of a CAR is through an ultrasonic flow system that utilizes sonoporation as a method of transfection. The sonoporation allows for a mechanical process to load the T-cells with the CAR (Figure 3)

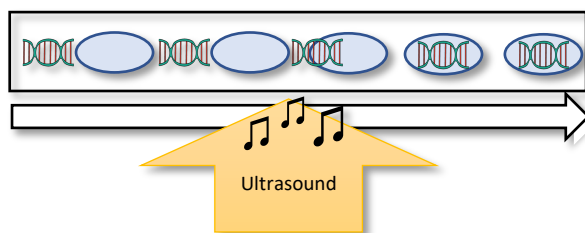


*Figure 3: A combination flow/sonoporation system could be used as a transfection method for loading CARs into T-cells. This process is non-viral and shows potential consistency benefits.*

[28]. A device to test this method was created in Dr. Jonathan Kopechek's laboratory at the University of Louisville prior to the beginning of this thesis. Previous to the fabrication of the device, this sonoporation process was conducted in a bulk setup. A clinical ultrasound probe was aimed at a conical tube in a water tank (for coupling purposes) and the cells were treated with ultrasound waves. This set up resulted in inconsistent ultrasound exposure and shielding of a portion of the cells caused by the microbubbles closer to the ultrasound source attenuating ultrasound waves before reaching cells further away from the source. To fix this issue and add consistency to the treatment, a microfluidics device



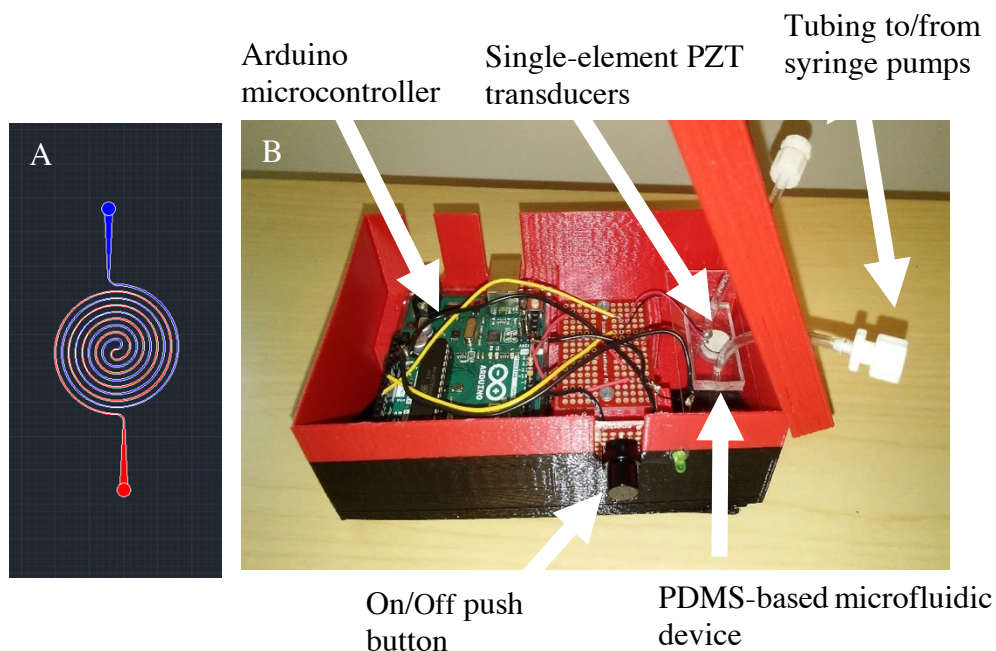
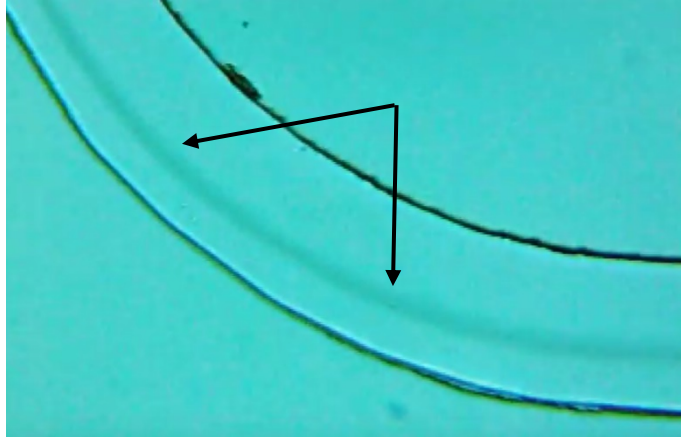


Figure 4: (A) Microfluidics device design that is in ultrasonic flow system. The channel width is 500 microns. (B) Ultrasonic flow device created in Dr. Jonathan Kopechek's laboratory. The device includes an integrated PZT transducer that applies ultrasound directly to the cells flowing through the microfluidics setup within the device.

was implemented into the sonoporation process. After testing a multitude of designs, a concentric circle was decided upon for the microfluidic channels (Figure 4-5). This design prolongs the exposure the cells receive to the ultrasound waves. To avoid using a clinical probe to treat the cells, a PZT ultrasound transducer was attached directly to the microfluidics device (Figure 5). The ultrasound transducer is microcontroller-driven, which has been set up next to the microfluidics device. The Arduino, circuit board, and microfluidics device were then encased in a 3D-printed container that included holes for the tubing, power cords, and power button. When using this device to process, the cells are pumped using a syringe pump (not shown in Figure 5) into the tubing. The cells, microbubbles, and desired loading molecule flow through the entrance tubing (Figure 5), into the microfluidics device where they are exposed to the ultrasound waves, and out the exit tubing to be collected in a vial for post-treatment assessment.



*Figure 5: Microscopy image of red blood cells flowing through a microfluidics device. The arrows point to the stream of red blood cells.*

This device allows for versatility as the microfluidics design can be adjusted along with the ultrasound and flow parameters. With some additional effort, the device can be optimized to load a multitude of cell types with many different small molecules [28]. To date, cancer cells, red blood cells, and immune cells have been processed in this specific device. With effort to optimize the necessary parameters, this ultrasonic flow system could be a non-viral alternative for transfection of T-cells for CAR-T therapy.

#### *CAR-T Shortcomings and Room for Improvement*

The current pipeline for CAR-T treatment is lengthy and has opportunity for improvement. As is, blood collection from the patient takes place which includes all blood cell types. T-cell isolation and activation occurs in order to separate out the T-cells for further engineering. This process includes the introduction of magnetic beads with CD3 and CD28 antibodies onto the T-cells. The now-isolated cells are then engineered through viral transduction so that they will express the sought-after CAR. The T-cells must then be multiplied ex-vivo for 10-14 days to reach the therapeutically necessary number of cells. Often  $10^9$  to  $10^{10}$  T-cells are required for the transfusion to work. After expansion, the

magnetic beads are removed from the cell solution and prepared for transfusion. To precondition the patient for receiving the treatment, they must receive conditional chemotherapy drugs shortly before transfusion [32].

Most medical centers do not have the GMP-compliant facilities to conduct this process. Therefore, cells needing to be processed must be stored through refrigeration or freezing and shipped to processing facilities, processed, stored again, and shipped back to the hospital. This lengthy process can cause unwanted phenotypical changes in the T-cells and can take several weeks for the patient to receive their treatment [33, 34].

Several severe challenges also limit the safety and availability of this treatment in patients. Some adverse symptoms seen include cytokine release syndrome and neurotoxicity [20, 21]. This random retroviral approach has resulted in the creation of an oncogene in some studies [16, 17]. It is thought that these symptoms are a result of the variability in CAR expression. Currently, lentiviral or retroviral vectors are primarily used for CAR expression. Although this creates a permanent modification to the gene, this approach has its drawbacks as the CAR-expressing gene is randomly inserted into the genome [20, 21]. A more consistent and direct method of loading the CAR into T-cells would be beneficial to patient success. Therefore, we hypothesized that the use of microfluidic sonoporation will increase the efficiency and consistency of T-cell transfection.

## II. PROCEDURE

### *Fabrication/Setup of Device*

A 3-inch silicon wafer coated with SU-8 was produced in a clean room by a standard photolithography process to generate the master design. PDMS (SylGard 184 Silicone Elastomer Kit (Dow Corning - 184 SIL ELAST KIT 0.5KG) was mixed and poured over the wafer in a petri dish. The PDMS was baked in a laboratory oven to cure, cut to size, and hole punched. The PDMS devices were then plasma-bonded on glass slides (MilliporeSigma, Burlington, MA, USA) and tubing was added. The PZT transducer (StemInc, Millbrae, CA, USA) was attached directly to the bottom of the microfluidics device and positioned in the 3D printed case. An Arduino Uno microcontroller (Arduino, Somerville, MA, USA) was programmed and wired in the case to drive the transducer. The Arduino was plugged in and a syringe with cell solution was connected to the input side of the tubing and controlled by air pressure from an empty 60 mL syringe using an Aladdin syringe pump (Aladdin Single-Syringe infusion Pump, World Precision Instruments, LLC, Sarasota, FL, USA). The output was connected into a collection vial and the device was ready for cell processing.

### *A549 Cell Culture and Harvesting*

A549 cells were cultured in complete DMEM media (10% fetal bovine serum, 1% penicillin/streptomycin) (VWR, Radnor, PA, USA) at 37 °C and 5% CO<sub>2</sub>. Before harvesting, the cells were washed once with PBS. Trypsin (0.25%) EDTA (VWR, Radnor, PA, USA) was added to release the adherent cells and incubated for 5 minutes. The solution was neutralized with complete media, collected in a conical tube, and centrifuged at 1500g for 5 minutes at 4 °C. The cells were resuspended at a concentration appropriate for the experiment.

### *Primary T-Cell Isolation*

The peripheral blood mononuclear cell (PBMC) samples were kept at -150 °C for storage. After retrieval, the frozen vials were quickly thawed in a water bath at 37 °C. The cells were diluted 1:10 in PBS, transferred to a 15-mL conical, and centrifuged at 580g at 4 °C for 11 minutes. The supernatant was aspirated, and 13 mL of autoMACS running buffer was added (MACS Miltenyi Biotec, Bergisch Gladbach, Germany). The cells were counted using an automated cell counter. The cells were centrifuged again, and the supernatant was aspirated. While keeping the solutions cold, the cells were resuspended in 40 µL of running buffer per 10 million cells. 10 µL of Pan T-Cell Biotin Antibody Cocktail was added per 10 million cells (MACS Miltenyi Biotec, Bergisch Gladbach, Germany) for isolation of T-cells. The cells were mixed well and incubated at 4 °C for 5 minutes per 10 million cells. 30 µL of buffer and 20 µL of Pan T-Cell MicroBead Cocktail was added per 10 million cells (MACS Miltenyi Biotec, Bergisch Gladbach, Germany). The cells and beads were mixed well and incubated for an additional 15 minutes at 4 °C. Rinsing buffer was added to make the total volume 500 µL. The cells were separated using an autoMACS Pro Separator (MACS Miltenyi Biotec, Bergisch Gladbach, Germany) using the “depletes separation” setting. The cells were counted again using an automated cell counter. The cells were diluted in 10 mL PBS and centrifuged. The supernatant was aspirated, and the cells were resuspended in 1 mL PBS and counted again. The cells were then aliquoted into the appropriate amount of microcentrifuge tubes, the plasmid or fluorescein was added, and experiments were conducted.

### *Microbubble synthesis*

Microbubbles were synthesized as previously described in Kopechek, *et al.*, 2015 for studies involving ultrasound treatment [30]. The microbubbles were composed of a gas perfluorocarbon core surrounded by a lipid shell. Cationic microbubble lipid solution was

composed of 100:43:1:4.5 molar ratio (DSPC:DSEPC:DSPG:PEG-40). Neutral microbubble lipid solution was composed of 96:4 molar ratio of DPPC:DSPE-PEG2000. All phospholipids were obtained from Avanti Polar Lipids (Alabaster, AL, USA) except for polyethylene glycol-40 stearate (Sigma-Aldrich, St. Louis, MO, USA). Lipids were dissolved in chloroform and the solvent was evaporated under argon. The dry lipid film was rehydrated in phosphate buffered saline (PBS) to a concentration of 10 mg/mL and sonicated with a probe sonicator to disperse the lipids.

To produce microbubbles, the prepared lipid solution was diluted 4x in PBS in a clear 11mm glass crimp vial and sealed with a 10mm target septa and 11mm taponos crimp (VWR, Radnor, PA, USA). The remaining air in the vial was replaced with decafluorobutane (Fluoromed, Round Rock, TX, USA) via a 20G hypodermic needle (Becton Dickinson, Franklin Lakes, NJ, USA) and a second needle to vent. The vial was then mixed by a high-speed amalgamator for 30 s at 4350 CPM (Pelican).

#### *Bacteria Growth and GFP Plasmid Isolation*

Luria broth (LB) was prepared by combining NaCl, Tryptone, and Yeast Extract in a 2:2:1 ratio in distilled water. Ampicillin was added right before culture growth began. Using a sterile pipette tip, a single colony (CMV promoter, ampicillin resistant, cat. no. 11153 from Addgene, Watertown, MA, USA) was selected from the LB agar plate and dipped into the LB plus antibiotics mixture and swirled. The culture was covered and allowed to incubate at 37 °C for 12-18 hours in a shaking incubator. The bacteria were then harvested by centrifugation at 1500g for 5 minutes. The supernatant was removed, and the bacteria were resuspended, lysed, and neutralized. The supernatant was then transferred to a Thermo Scientific GeneJET Spin Column and centrifuged for 1 minute and then washed twice, centrifuging for 30-60 s each time. The column was transferred to a new tube and Elution Buffer was added. The DNA was

incubated and centrifuged for at 1500g for 2 minutes and the flow-through was collected (protocol from Thermo Scientific GeneJET Plasmid Miniprep Kit, Thermo Fisher Scientific, Waltham, MA, USA). Plasmid concentrations were quantified with a NanoDrop 2000C (Thermo Fisher Scientific).

#### *Lipofectamine-3000 Experiments*

Adherent cells were plated in advance and 70-90% confluent at the time of transfection. Primary suspension cells were isolated prior to transfection. Transfection by Lipofectamine-3000 was completed according to Thermo Fisher Scientific's supplied protocol (Waltham, MA, USA) using serum-free medium. GFP plasmid (Addgene, Watertown, MA, USA) dosages ranged between 250 ng to 1 µg per sample and incubated for 48 hours before analysis. Flow cytometry analysis was then performed.

#### *Electroporation*

A Neon Transfection System and kit was used for electroporation (Thermo Fisher Scientific). Cells were washed, trypsinized, neutralized, and counted prior to electroporation process. Cells were centrifuged (1500g for 5 minutes at 4 °C for A549 cells; 580g for 10 minutes at 4 °C for T-cells), supernatant was aspirated, and cells were resuspended in 100 µL recommended resuspension buffer (buffer R for A549 cells, buffer T for T-cells) at a density of  $1.0 \times 10^7$  cells/mL. GFP plasmid (Addgene, Watertown, MA, USA) was added to the cells at a concentration of 25 ng/µL. Fluorescein was added at 0.1 mg/mL concentration. Electroporation was conducted following the supplied protocol (Thermo Fisher Scientific). A549 cells and T-cells were transfected using the following parameters, respectively: 1230V, 30ms, 2 pulses and 500V, 20ms, 1 pulse. The transfected cells were allowed 48 hours for expression after plasmid transfection and analyzed by flow cytometry. Cells exposed to fluorescein were washed in flow tubes immediately after electroporation and analyzed by flow cytometry.

### *Sonoporation*

The cells were collected and washed. The prepared microbubbles were added at cells:microbubble ratios (199:1, 99:1, 65.7:1, 49:1, 39:1, 19:1) and incubated 1-2 minutes. The GFP plasmid (1 µg/mL) (Addgene, Watertown, MA, USA) or fluorescein (0.1 mg/mL) (MilliporeSigma, Burlington, MA, USA) was then added to the samples and passed through a microfluidic device with a channel diameter of 550 µm at a rate of 30-60 mL/h. Ultrasound was applied through an integrated transducer at a pressure of 0.1-0.5 MPa. If fluorescein was used, the samples were kept in fluorescein during the processing for 10 minutes (both control and sonoporated samples) and washed in flow cytometry tubes directly after. If transfected, the cells were collected and plated for 24-72 hours to allow time for the GFP plasmid to be internalized and expressed. The primary T-cells were activated during this time (Dynabeads™ Human T-Activator CD3/CD28 for T Cell Expansion and Activation, Thermo Fisher Scientific, Waltham, MA, USA). Flow cytometry analysis was then performed.

### *Flow Cytometry Analysis*

Transfection and loading efficiency were determined through the detection of GFP plasmid (Addgene, Watertown, MA, USA) expression or fluorescein uptake via a flow cytometer (MACSquant, Miltenyi Biotec, Germany; BD FACSCANTO II, BD FACSCalibur, Franklin Lakes, NJ, USA). Data was analyzed using flow cytometry software (FlowJo, Ashland, OR, USA). The live cells were gated out by the distribution by forward and side scattering. From there, the FITC fluorescence intensity was graphed in a histogram (x-axis displaying the logarithmic fluorescence intensity value and y-axis displaying the cell count) and the mean fluorescence intensity was obtained by the histogram. These intensities were averaged if the sample size was larger than one and standard deviations were calculated using Microsoft Excel 2016 (Microsoft, Redmond, WA, USA).



*Statistical Analysis*

Statistical comparisons between experimental and control groups were determined using a Student's t-test, with statistical significance ( $p < 0.001-0.05$ ) defined under each figure.

Bars represent mean  $\pm$  standard error.

### III. RESULTS AND DISCUSSION

#### *Fluorescein Loading Studies*

#### *Sonoporation Microbubble Dose Study*

Cells were sonoporated with fluorescein in the solution to assess the uptake of small fluorescent molecules.

A range of microbubble volumes were tested. Although the differences seem negligible

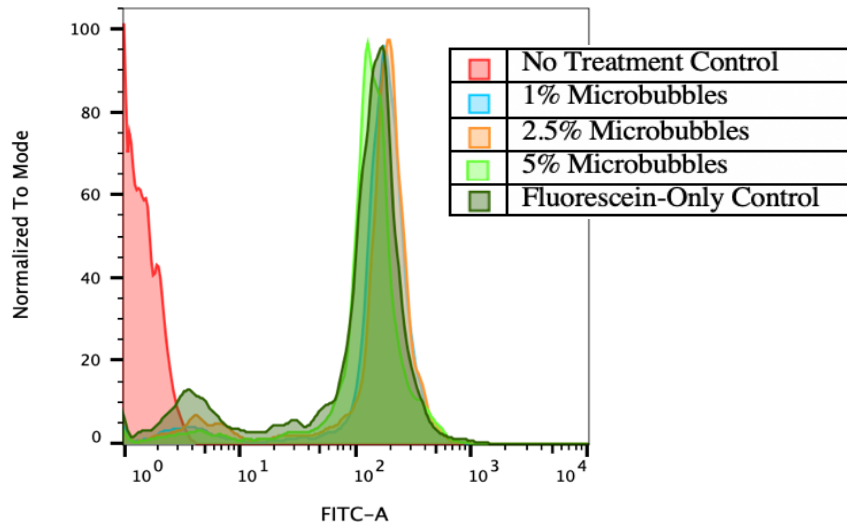


*Figure 6: Multiple cationic microbubble doses were tested for their sonoporation loading efficiencies on primary T-Cells. The results were assessed by flow cytometry. (N=1)*

based on the histogram analysis, the 2.5% v/v dose (orange histogram peak) seems to have the highest fluorescence value (Figure 6). When graphed, the mean fluorescence intensity

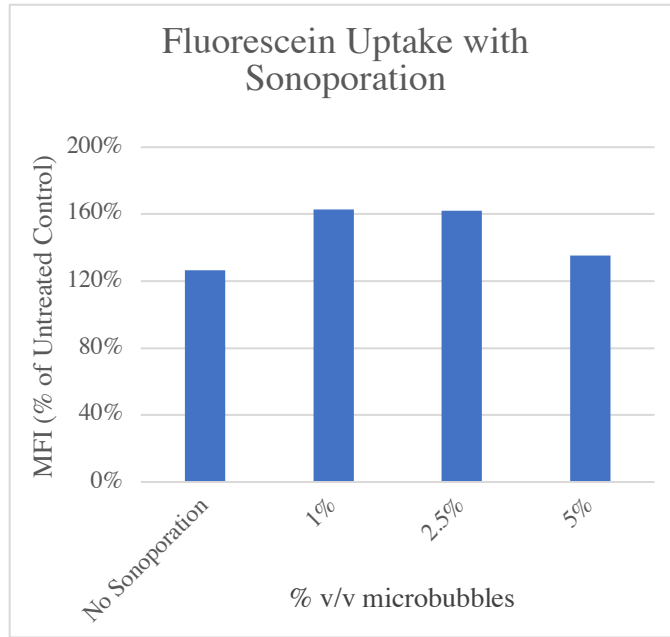


Figure 7: Multiple cationic microbubble doses were tested for their sonoporation loading efficiencies on primary T-Cells. The results were assessed by flow cytometry. (N=1)

was shown to be the highest in the 1% and 2.5% microbubble doses (Figure 7). This sample set had N=1 but this correlates with prior results that were collected from the loading of fluorescein into red blood cells using sonoporation (Figure 8). This sonoporation was conducted using a clinical ultrasound probe and water tank but the optimal bubble dose remains the same. This indicates the importance of the microbubble concentration within the solution.

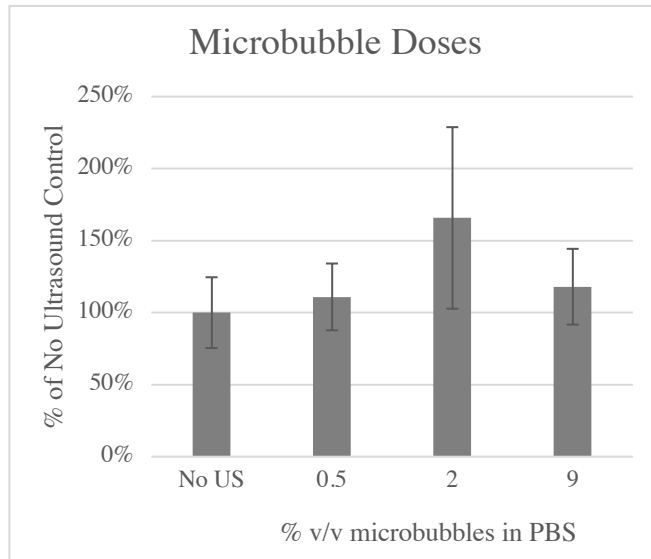


Figure 8: Multiple cationic microbubble doses were tested for their sonoporation loading efficiencies on red blood cells. The results were assessed by flow cytometry and the mean fluorescent intensity (normalized to no treatment control) was graphed. The cells were treated with a clinical ultrasound probe (Verasonics P4-1 transducer) at 20V, 0.1 ms pulse, 20 mL/hour flow rate in a 200  $\mu$ m width microfluidics device channel. (N=4)

### Other Transfection Method Assessment of Fluorescein Uptake

Uptake of fluorescein by electroporation was tested alongside the sonoporation data for comparison. No increase in fluorescence was detected in the first sonoporation

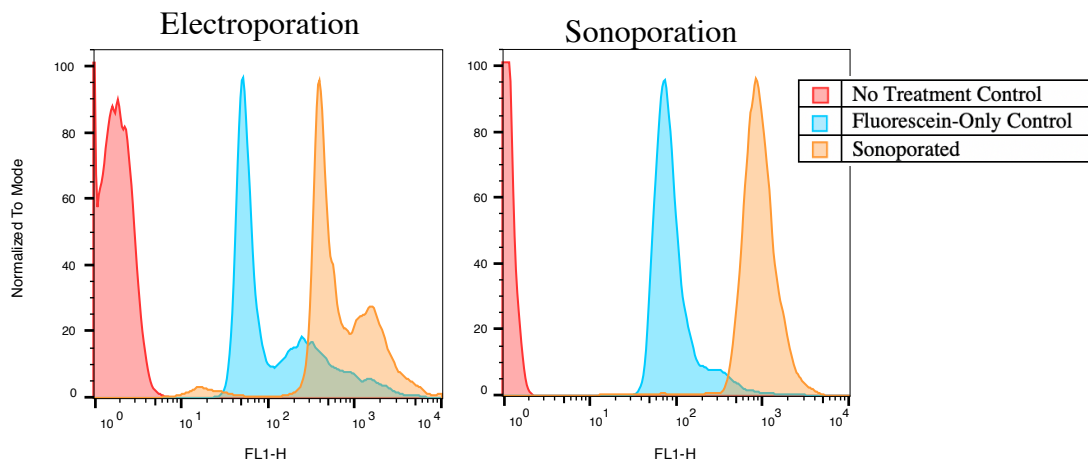
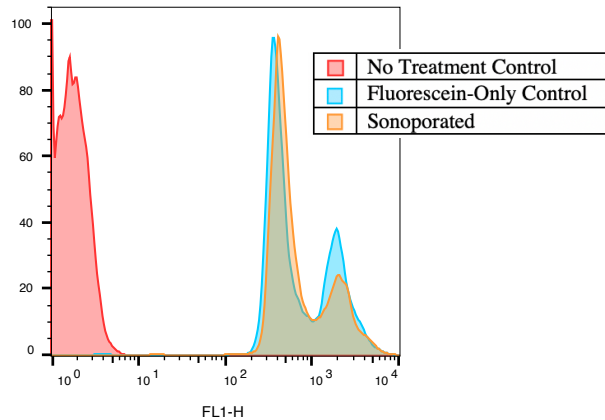


Figure 9: Primary T-cells were loaded with electroporation (left) and sonoporation (right) and assessed using flow cytometry. (N=3)

experiment (Figure 10). Due to the high amount of fluorescence intensity in the non-sonoporated fluorescein control, it was hypothesized that the uptake was saturated by the nonspecific uptake of the fluorescein. The non-sonoporated fluorescein-only control



*Figure 10: Primary T-Cells were loaded with sonoporation and assessed using flow cytometry. Fluorescein control procedure was adjusted to minimize nonspecific uptake of fluorescein. (N=3)*

samples had fluorescein in the solution while the treated samples were being sonoporated. This was enough time for the cells to nonspecifically take in their maximum amount of fluorescein. To avoid this issue, experiments were repeated where the non-sonoporated fluorescein-only controls were left in the fluorescein for less time than in the initial experiment. The cells only remained in fluorescein for as long as it took to sonoporate one sample (approximately 11 minutes) and were washed immediately after. A large increase could then be detected in the loaded sample when compared to the fluorescein-only sample (Figure 9). When the mean fluorescence was graphed, there was a 3.5-fold increase in the electroporated sample in comparison to the non-electroporated fluorescein-only control and a 5-fold increase in the sonoporated sample in comparison to its fluorescein-only control (Figure 11). These increases were significant with a p-value of less than 0.05. The

decrease in the fluorescein-only control group's fluorescence intensity in comparison to Figure 10 shows that the hypothesized issue of letting the cells rest in fluorescein too long was accurate. An adjustment to the protocol allowed for a difference in fluorescence intensity to be measured while using sonoporation as a loading method for fluorescein.

When the electroporation and sonoporation results were compared, the sonoporation method was more successful at loading the primary T-cells with fluorescein. The sonoporated sample took in 34% more fluorescein than the electroporated sample. These results are trending towards significance with a current p-value of 0.137 (Figure 11). Additionally, two populations can be detected in the electroporation curve but not in the sonoporation curve. The two populations indicate a low loading level and a high loading level. Ultimately, if the same populations are seen with transfection, this could cause an inconsistent loading of the CAR gene, leading to variability in expression levels of the CAR. This data indicates that sonoporation may cause more consistent loading which would help

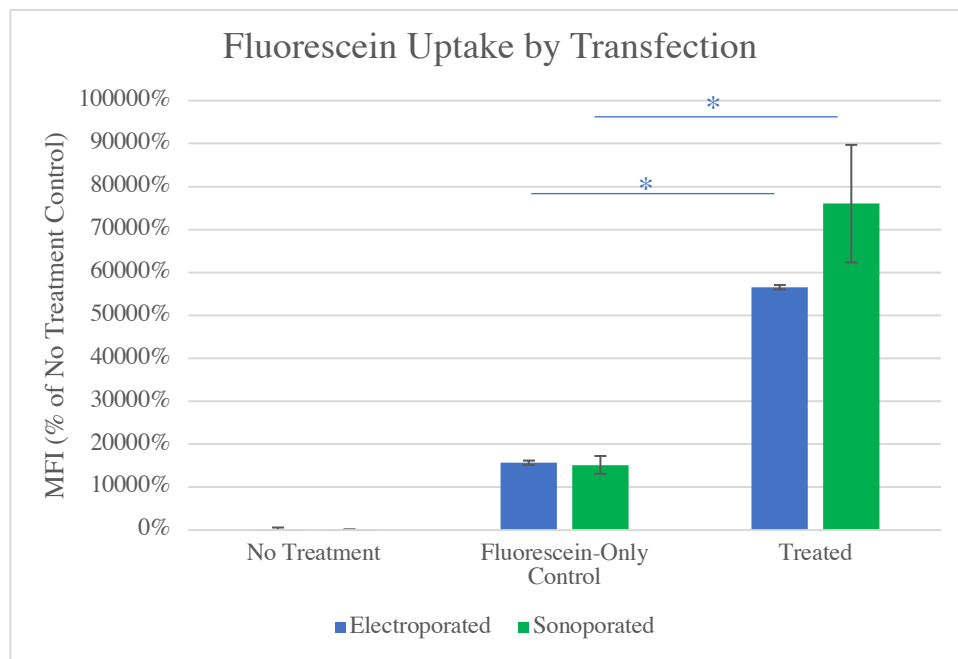


Figure 11: Primary T-Cells were loaded with electroporation and sonoporation and assessed using flow cytometry. (\* $p < 0.05$ ) (N=3)

avoid the unwanted side effects that come from uneven CAR expression, such as cytokine release syndrome and tumor lysis syndrome. Although electroporation has been considered the more efficient non-viral transfection method for primary T-cells, these results suggest that sonoporation may actually cause higher, more consistent loading for small molecules [35]. A higher sample size of this data set would be necessary to conclude significance.

### *Immune Cell Model Investigation*

Additional studies were performed to test loading efficiency in jurkat cells by means of electroporation to determine if they were an equivalent model for primary T-cells. After electroporation with fluorescein and flow cytometry analysis, there was a negligible shift measured in the jurkat cells between the fluorescein only control and loaded samples (Figure 12). In comparison, there was a noticeable shift by the primary T-cells when comparing the loaded group to the fluorescein-only control group. To further investigate, the mean fluorescence intensities were graphed (Figure 13). There is a 2-fold

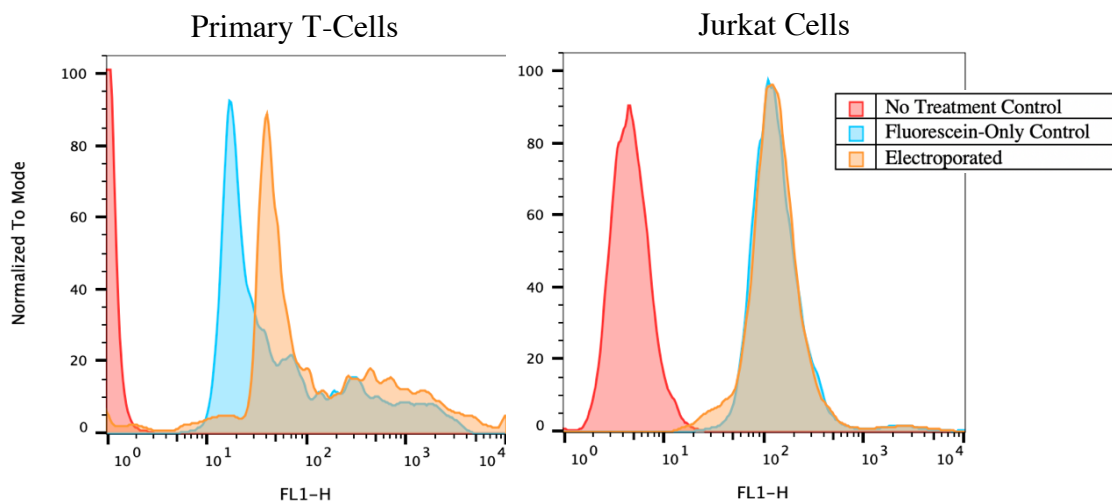


Figure 12: Primary T-Cells and jurkat cells were loaded with electroporation and analyzed by flow cytometry. (N=1)

increase in fluorescence intensities between the electroporated primary T-cells and the fluorescein-only control. The difference is undetectable in the jurkat cells. This not only aligned with the previously discussed electroporation experiment, but it also shows that jurkat cells are not an equivalent model for primary T-cells.

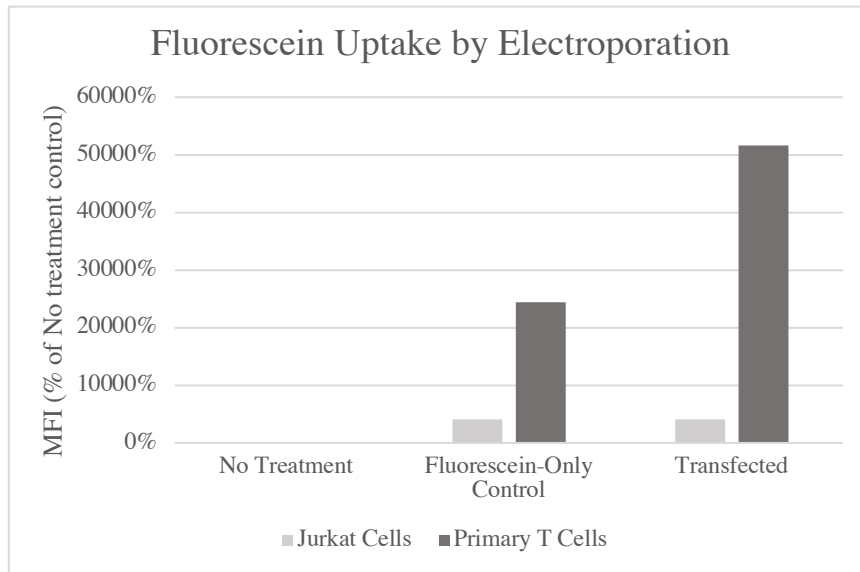


Figure 13: Primary T-Cells and jurkat cells were loaded with electroporation and analyzed by flow cytometry. (N=1)

### *GFP Plasmid Transfection Studies*

#### *Sonoporation Microbubble Composition Study*

Sonoporation was then tested for its ability to transfect cells with GFP plasmid. Primary T-cells were transfected with GFP plasmid by means of sonoporation using 2.5% microbubbles % v/v in each sample. At 24 hours, a slight increase in fluorescence could be distinguished in the cationic microbubble histogram when compared to the control and neutral microbubble samples (Figure 14). The mean fluorescence intensities of each sample



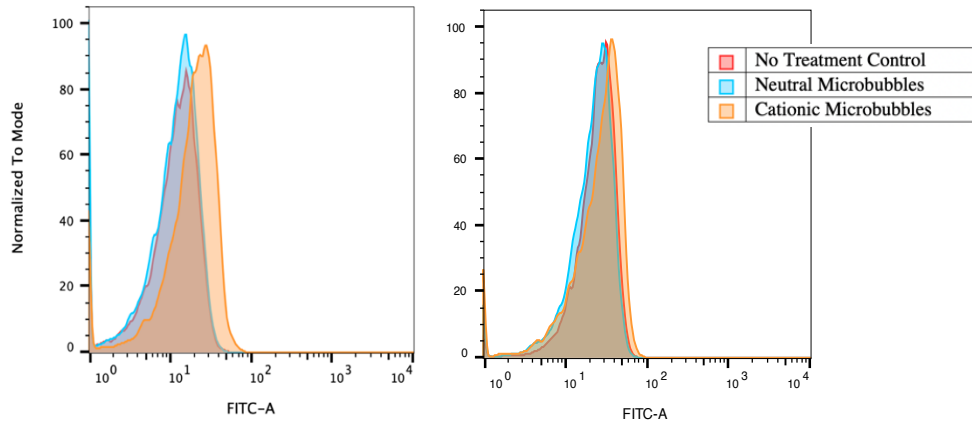


Figure 14: Primary T-cells were transfected with GFP plasmid by means of sonoporation and activated. Flow cytometry was run 24 (left) and 48 hours (right) after treatment. N=1

were graphed. It can again be determined that the most GFP plasmid was expressed (166% of neutral bubble uptake) when using cationic bubbles for sonoporation and activating the T-cells for 24 hours before assessment (Figure 15). Although sample sizes were low, these results are consistent with expected results since the cationic bubbles interact more closely with the cells which is expected to increase the efficiency of sonoporation.

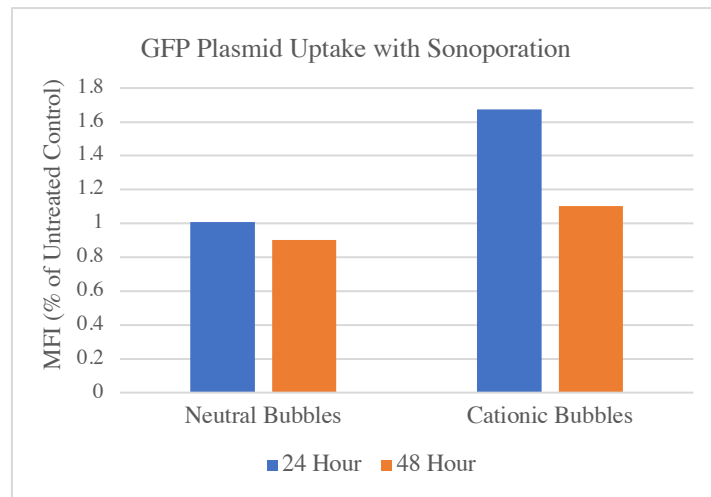


Figure 15: Primary T-cells were transfected with GFP plasmid by means of sonoporation and activated. Flow cytometry was run 24 (left) and 48 hours (right) after treatment and mean fluorescence was graphed. N=1

### Sonoporation T-cell Activation Timepoint Studies

Activation times were explored to understand when the most GFP plasmid was expressed in the transfected T-cells. The tested time points included 14, 24, 48, and 72 hours. An increase in fluorescence intensity was indistinguishable for the first three time points (Figure 16-17). It was not until the 48-hour activation time that a shift in the fluorescence could be detected (Figure 17).

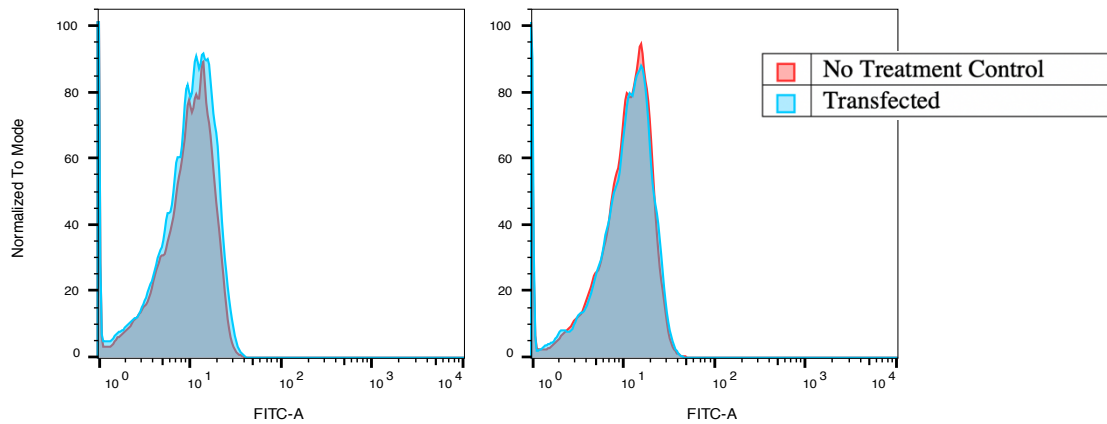


Figure 16: Primary T-cells were transfected with GFP plasmid by means of sonoporation and activated. Flow cytometry was run 14 (left) and 24 hours (right) after treatment. Microbubbles were cationic. N=1

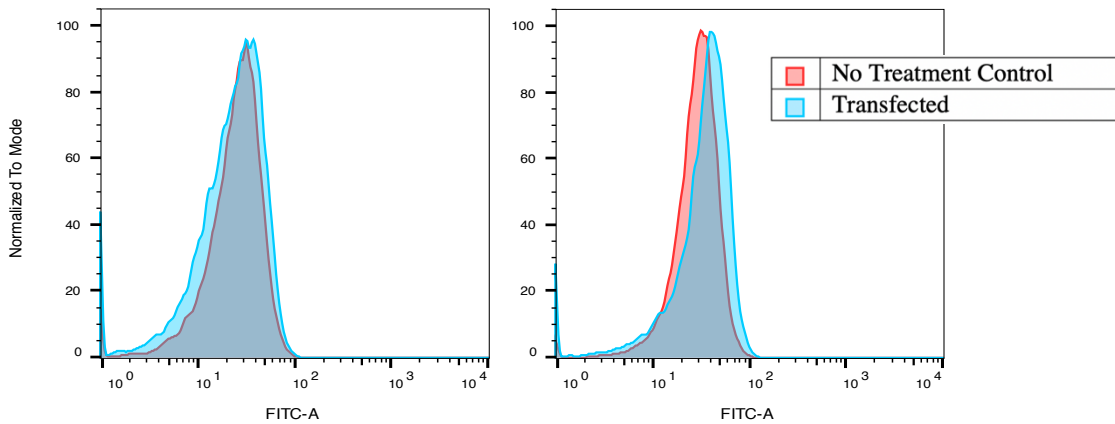


Figure 17: Primary T-cells were transfected with GFP plasmid by means of sonoporation and activated. Flow cytometry was run 48 (left) and 72 hours (right) after treatment. Microbubbles were cationic. N=1

The mean fluorescent intensity results from each timepoint experiment were normalized to the no treatment controls and combined in Figure 18. From experiment 1, it can be concluded that the most GFP plasmid was expressed at 24 hours (Figure 18). This was not replicated, however, when experiment 2 was conducted. The 72-hour timepoint resulted in the most consistent fluorescence intensity values. Repetitions of the timepoint study would be necessary for drawing stronger conclusions. As seen in the figure, the experiments were conducted with low sample sizes. Overall though there does not appear to be a significant difference at these time points.

#### *Sonoporation Transfection of A549 Cells*

Uptake and expression of GFP plasmid by sonoporation transfection methods was assessed in human lung cancer cells at 48 hours by flow cytometry. No significant difference was detected between the control and transfected samples (Figure 19). Although

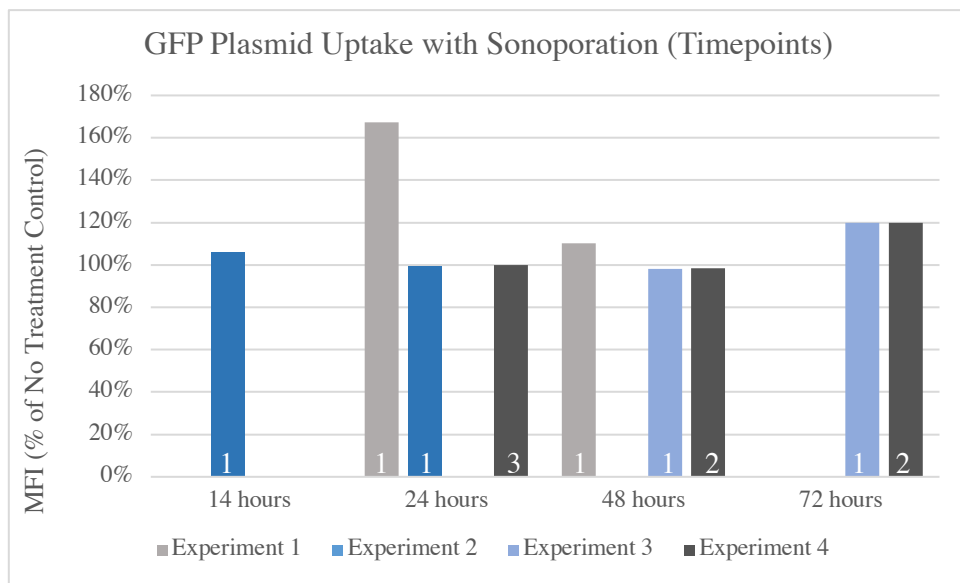
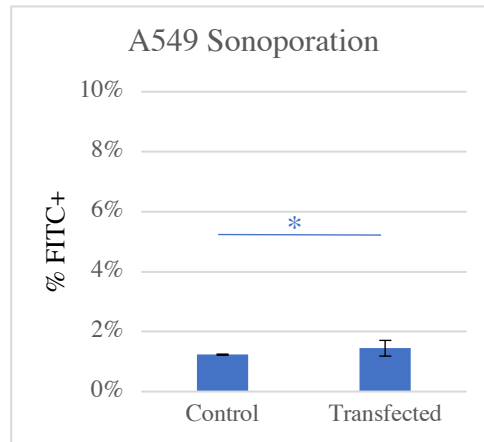


Figure 18: Primary T-cells were transfected with GFP plasmid by means of sonoporation and activated. Timepoint data was combined from four different experiments. The results were assessed by flow cytometry. White number in bar represents number of replicates for each experiment.

sonoporation proved its success at loading smaller molecules such as fluorescein, the lack of success in plasmid transfection suggests that it may not be the best method of loading larger molecules such as plasmids.



*Figure 19: Sonoporation transfection was quantified through %FITC+ cells detected in the sample by flow cytometry. No significant difference was detected in the fluorescent levels of the control vs. transfected samples. (\* $p < 0.05$ ) (N=2-3)*

The lack of success in transfected A549 cells through means of sonoporation however, could also be explained by the lack of optimization. The ultrasound parameters, microbubble dose, or plasmid concentration may not have been effective for transfection of these cells. Sonoporation has proven success as a transfection method in other studies [36, 37], so future studies with optimized parameters are expected to have higher levels of transfection. To prove that these cells could be transfected with more standard methods of transfection, other approaches were tested for comparison with the sonoporation results.

### *Lipofectamine Transfection*

Uptake and expression of GFP plasmid by Lipofectamine 3000 transfection methods was assessed in primary T-cells and A549 (lung carcinoma) cells at 24 hours by

flow cytometry (Figure 20). A significant 50-fold increase ( $p < 0.001$ ) in %FITC+ cells was detected in the transfected cancer cells compared to the non-transfected control group while

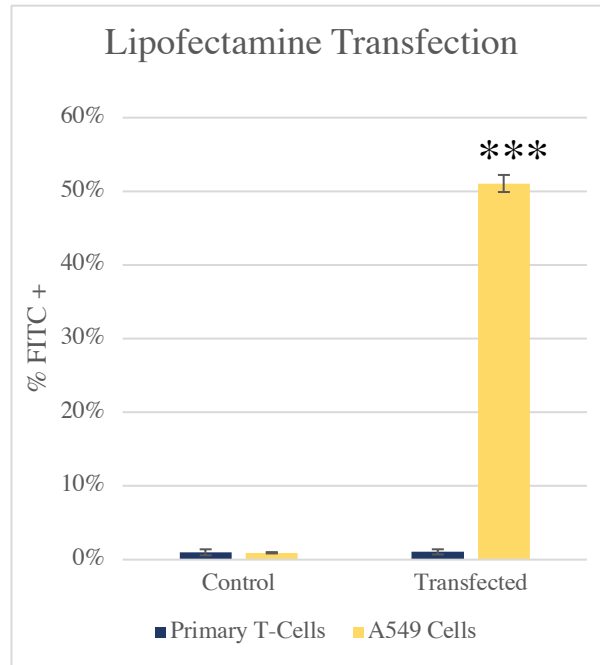


Figure 20: Lipofectamine 3000 transfection was quantified through percentage of FITC + cells detected in the sample by flow cytometry. A 50-fold increase was detected in human lung cancer cells while no difference was detected in human T-cell uptake. (\*\*\*) indicates  $p < 0.0001$  ( $N=3$ ).

no identifiable difference was presented in the T-cells (Figure 20). This indicates that Lipofectamine3000 may be more successful at transfecting cancer cells when compared to primary T-cells.

### *Electroporation Transfection*

The mean FITC intensity was evaluated and displayed as histograms for both cell types (Figure 21). The significant right shift in fluorescence proves the successful transfection in the human lung cancer cells by means of electroporation. The lack of shift

in the T-cell histogram further proves the failure to transfect these cells using the described technique in Zhang, *et. al.* 2018. This paper loaded 1  $\mu\text{g}$  plasmid while 2.5  $\mu\text{g}$  were loaded here but the parameters stayed the same. The present study failed to replicate the published data which reported nearly 60% transfection efficiency with a 3-day post-treatment incubation [38].

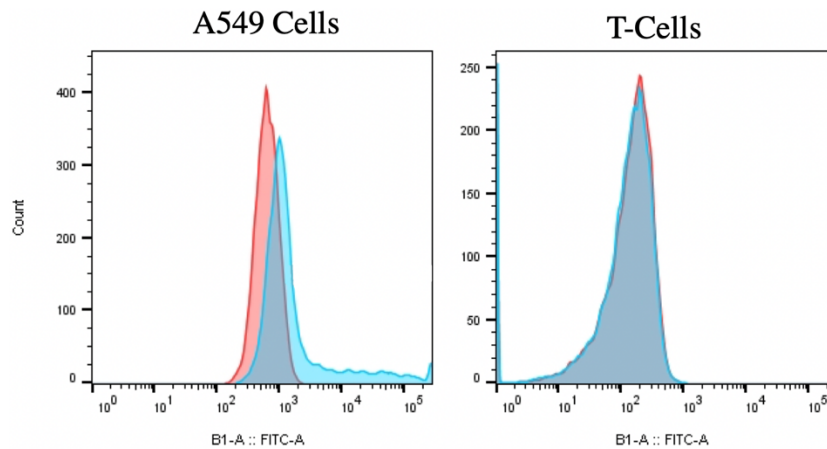


Figure 21: The FITC histograms displayed show the shift in fluorescence between the control (red) and transfected (blue) samples. The mean intensity of the T-cell fluorescence did not shift after transfection. These cells were transfected using electroporation.

### *Microscopy Analysis*

#### *Microscopy Imaging of Electroporation Transfection*

Fluorescent microscopy was performed 48 hours after treatment to visualize GFP plasmid transfection efficiency with electroporation in human lung cancer cells and primary T-cells (Figure 22). There is a clear uptake and expression of the GFP plasmid by the cancer cells in the transfected group, shown by the green fluorescent cells detected by

fluorescent microscopy (Figure 22A-B). The same results were not seen in the primary T-cells (Figure 22C-D). This indicates that after 48 hours, transfection by electroporation was successful in the cancer cells and sufficient time was given for expression. This further proves the data discussed previously (Figure 21) that showed the same increase in fluorescence in the cancer cells.

#### *Microscopy Imaging of Lipofectamine 3000 Transfection*

Fluorescent microscopy was performed 24 hours after treatment to visualize GFP plasmid transfection efficiency with Lipofectamine 3000 in human lung cancer cells and T-cells (Figure 23). The uptake and expression of the GFP plasmid can be detected in the human lung cancer cells (Figure 23A-B); however, not in the human T-cells (Figure 23C-D). This indicates that after 48 hours, transfection by Lipofectamine 3000 was successful in the cancer cells and sufficient time was given for expression. This also further proves that as discussed with Figure 20, Lipofectamine 3000 may not be the best transfection method for primary T-cells.

The lack of success in transfecting the T-cells with electroporation and Lipofectamine 3000 further explains how difficult these cells are to transfect. Any success by sonoporation could show a promising future in using it as a non-viral transfection method for primary T-cells. Additionally, the differences in fluorescent levels visible in the microscopy images (Figures 22-23) and wider FITC histogram peaks (Figure 21) indicates variability in plasmid uptake among individual cells. This is not uncommon for current methods of transfection. Theoretically, sonoporation using a microfluidics

approach would introduce a transfection method that would decrease this variability present in other means of transfection.

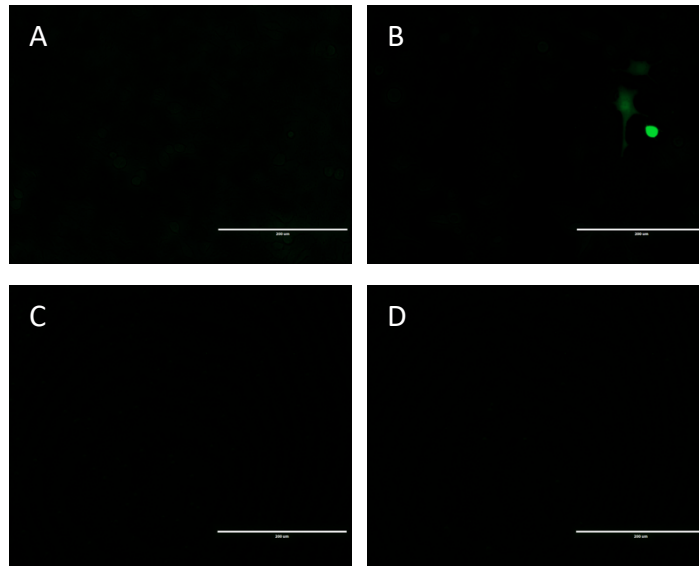


Figure 22(A,B): Electroporation transfection conducted in human lung cancer cells. Control cells (A), GFP plasmid transfected cells (B) dose =25 ng/ $\mu$ L.

Figure 22(C,D): Electroporation transfection conducted in human T-cells. Control cells (C), GFP plasmid transfected cells (D) dose =25 ng/ $\mu$ L.

Scale bar represents 200  $\mu$ m.

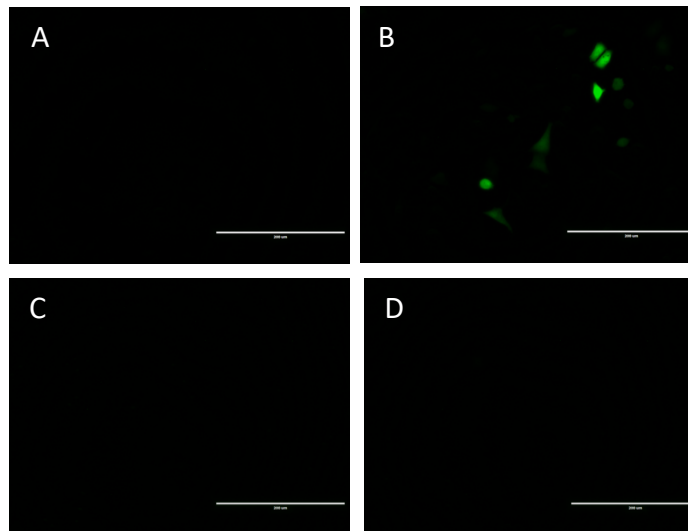


Figure 23(A,B): Lipofectamine 3000 transfection conducted in human lung cancer cells. Control cells (A), GFP plasmid transfected cells (B) dose =1ng/ $\mu$ L.

Figure 23(C,D): Lipofectamine transfection conducted in human T-cells. Control cells (C), GFP plasmid transfected cells (D) dose =1 ng/ $\mu$ L.

Scale bar represents 200  $\mu$ m.



#### IV. CONCLUSION

Based on the fluorescein studies, sonoporation is a promising method for loading primary T-cells with small molecules such as fluorescein. We also found that the incubation time for cells in fluorescein solutions affects the shift in fluorescence intensity seen on the histograms. Long incubation times can allow cells in the control groups to passively uptake high amounts of fluorescein which can make it difficult to detect differences in the treatment groups. It was also determined that Jurkat cells are not an equivalent model for primary T-cells. It can also be concluded that sonoporation is not as successful at transfecting primary T-cells with larger molecules such as GFP plasmid. This is most likely due to the size of the loading molecule and also the multiple steps and pathways involved from plasmid delivery to the production of fluorescent proteins in the cells.

Optimization of the sonoporation parameters would be necessary to improve the transfection efficiency of the primary T-cells. These parameters would include microbubble dose, flow rate, and ultrasound voltage, and possibly introducing pulsed ultrasound. It would also be beneficial to study a range of plasmid concentrations and activation timepoints. It is expected that these parameters need to be optimized for each cell type in order to experience the highest transfection efficiencies. Even though the current results do not show a large increase in GFP with sonoporation transfection, it is likely that further research and optimization will lead to improved sonoporation transfection efficiencies.

## V. RECOMMENDATIONS

Moving forward, more GFP plasmid loading experiments should be conducted to determine if sonoporation is an effective mode of transfection for T-cells. A range of ultrasound parameters (pressure and pulse iteration) in addition to flow rates and microbubble concentrations should be tested. Additionally, a range of GFP plasmid concentrations and activation timepoints should be studied. These experiments should be repeated for both technical replicates and experiment replicates to prove consistency in the results. While these are being run, the donor should remain the same. Once consistency is proven, transfection by sonoporation should be tested in a range of T-cell donors to make sure the results can be repeated in primary T-cells from different sources.

Once sonoporation and the loading of GFP plasmid is improved, the next step will be loading CARs into the primary T-cells and testing for their presence and ability to express the receptor. The specific insertion of the CAR into the genome can be improved by the addition of CRISPR-Cas9 into the transfection process. Ideally while this project advances, not only will sonoporation be established as the best method of non-viral transfection, but the expression consistency will be improved with the use of CRISPR-Cas9 to decrease unwanted symptoms of the CAR-T treatment and improve outcomes in patients.

## REFERENCES

1. Pui, C.H. and W.E. Evans, *Treatment of acute lymphoblastic leukemia*. N Engl J Med, 2006. **354**(2): p. 166-78.
2. Pui, C.H. *Acute Lymphoblastic Leukemia*. Encyclopedia of Cancer 2017; 2011:[]
3. Hunger, S.P., et al., *Improved survival for children and adolescents with acute lymphoblastic leukemia between 1990 and 2005: a report from the children's oncology group*. J Clin Oncol, 2012. **30**(14): p. 1663-9.
4. *Childhood Acute Lymphoblastic Leukemia Treatment*. 2018 [cited 2019 07]; 13]. Available from: [www.cancer.gov/types/leukemia/patient/child-all-treatment-pdq](http://www.cancer.gov/types/leukemia/patient/child-all-treatment-pdq).
5. Zelent, A., M. Greaves, and T. Enver, *Role of the TEL-AML1 fusion gene in the molecular pathogenesis of childhood acute lymphoblastic leukaemia*. Oncogene, 2004. **23**(24): p. 4275-83.
6. Arruga, F., et al., *Functional impact of NOTCH1 mutations in chronic lymphocytic leukemia*. Leukemia, 2014. **28**(5): p. 1060-70.
7. *Imatinib mesylate*. PubChem [cited 2019 07].
8. *Press Announcements - FDA Approval Brings First Gene Therapy to the United States*. Available from: [www.fda.gov/newsevents/newsroom/pressannouncements/ucm574058.htm](http://www.fda.gov/newsevents/newsroom/pressannouncements/ucm574058.htm).
9. Niederhuber, J.E., *Abeloff's Clinical Oncology: Fifth Edition*. 2013: Elsevier, Inc.
10. Jain, N., *Acute Lymphoblastic Leukemia in Adults*. Hematology: Basic Principles and Practice, 2013. **6**.
11. Harr, J., *Civil Action*. 1996: Vintage Books.

12. Lange, B.J., et al., *Double-delayed intensification improves event-free survival for children with intermediate-risk acute lymphoblastic leukemia: a report from the Children's Cancer Group*. *Blood*, 2002. **99**(3): p. 825-33.
13. Gragert, L., et al., *HLA match likelihoods for hematopoietic stem-cell grafts in the U.S. registry*. *N Engl J Med*, 2014. **371**(4): p. 339-48.
14. *Possible Side Effects of Mercaptopurine PO, Methotrexate PO*. 2014; Available from:  
<https://ctep.cancer.gov/protocolDevelopment/sideeffects/regimes/SideEffects-Mercapt-Methotrex-Pred-Vincrist.doc>.
15. Grupp, S.A., et al., *Chimeric antigen receptor-modified T cells for acute lymphoid leukemia*. *N Engl J Med*, 2013. **368**(16): p. 1509-1518.
16. Maude, S.L., et al., *Chimeric antigen receptor T cells for sustained remissions in leukemia*. *N Engl J Med*, 2014. **371**(16): p. 1507-17.
17. Maude, S.L., et al., *CD19-targeted chimeric antigen receptor T-cell therapy for acute lymphoblastic leukemia*. *Blood*, 2015. **125**(26): p. 4017-23.
18. Fesnak, A.D., C.H. June, and B.L. Levine, *Engineered T cells: the promise and challenges of cancer immunotherapy*. *Nat Rev Cancer*, 2016. **16**(9): p. 566-81.
19. Brentjens, R.J., et al., *CD19-targeted T cells rapidly induce molecular remissions in adults with chemotherapy-refractory acute lymphoblastic leukemia*. *Sci Transl Med*, 2013. **5**(177): p. 177ra38.
20. Bonifant, C.L., et al., *Toxicity and management in CAR T-cell therapy*. *Mol Ther Oncolytics*, 2016. **3**: p. 16011.

21. Davila, M.L., et al., *Efficacy and toxicity management of 19-28z CAR T cell therapy in B cell acute lymphoblastic leukemia*. *Sci Transl Med*, 2014. **6**(224): p. 224ra25.
22. Howard, S.C., D.P. Jones, and C.H. Pui, *The tumor lysis syndrome*. *N Engl J Med*, 2011. **364**(19): p. 1844-54.
23. Douglas, K.L., *Toward development of artificial viruses for gene therapy: a comparative evaluation of viral and non-viral transfection*. *Biotechnol Prog*, 2008. **24**(4): p. 871-83.
24. Rothe, M., A. Schambach, and L. Biasco, *Safety of gene therapy: new insights to a puzzling case*. *Curr Gene Ther*, 2014. **14**(6): p. 429-36.
25. DeBruin, K.A. and W. Krassowska, *Modeling electroporation in a single cell. I. Effects Of field strength and rest potential*. *Biophys J*, 1999. **77**(3): p. 1213-24.
26. Potter, H. and R. Heller, *Transfection by Electroporation*. *Curr Protoc Mol Biol*, 2018. **121**: p. 9 3 1-9 3 13.
27. Zhao, D., et al., *A Flow-Through Cell Electroporation Device for Rapidly and Efficiently Transfecting Massive Amounts of Cells in vitro and ex vivo*. *Sci Rep*, 2016. **6**: p. 18469.
28. van Wamel, A., et al., *Vibrating microbubbles poking individual cells: drug transfer into cells via sonoporation*. *J Control Release*, 2006. **112**(2): p. 149-55.
29. Fan, Z., R.E. Kumon, and C.X. Deng, *Mechanisms of microbubble-facilitated sonoporation for drug and gene delivery*. *Ther Deliv*, 2014. **5**(4): p. 467-86.

30. Kopechek, J.A., et al., *Ultrasound Targeted Microbubble Destruction-Mediated Delivery of a Transcription Factor Decoy Inhibits STAT3 Signaling and Tumor Growth*. *Theranostics*, 2015. **5**(12): p. 1378-87.
31. Hu, Y., J.M. Wan, and A.C. Yu, *Membrane perforation and recovery dynamics in microbubble-mediated sonoporation*. *Ultrasound Med Biol*, 2013. **39**(12): p. 2393-405.
32. Almasbak, H., T. Aarvak, and M.C. Vemuri, *CAR T Cell Therapy: A Game Changer in Cancer Treatment*. *J Immunol Res*, 2016. **2016**: p. 5474602.
33. Ramachandran, H., et al., *Optimal thawing of cryopreserved peripheral blood mononuclear cells for use in high-throughput human immune monitoring studies*. *Cells*, 2012. **1**(3): p. 313-24.
34. Sadeghi, A., et al., *Rapid expansion of T cells: Effects of culture and cryopreservation and importance of short-term cell recovery*. *Acta Oncol*, 2013. **52**(5): p. 978-86.
35. Riedl, S.A.B., *Non-Viral Transfection of Human T Lymphocytes*. *Processes*, 2018.
36. Bao, S., B.D. Thrall, and D.L. Miller, *Transfection of a reporter plasmid into cultured cells by sonoporation in vitro*. *Ultrasound Med Biol*, 1997. **23**(6): p. 953-9.
37. Tlaxca, J.L., et al., *Analysis of in vitro transfection by sonoporation using cationic and neutral microbubbles*. *Ultrasound Med Biol*, 2010. **36**(11): p. 1907-18.
38. Zhang, Z., et al., *Optimized DNA electroporation for primary human T cell engineering*. *BMC Biotechnol*, 2018. **18**(1): p. 4.

## VITA

Emily Murphy received her Bachelor of Science in Bioengineering from the University of Louisville in 2018. In 2016, she began her co-op career under Dr. Jonathan Kopechek and Dr. Tariq Malik, located primarily in the Clinical and Translational Research Building. Her focus was in a cancer-targeting nanoemulsions project utilizing the aptamer AS1411. Her following co-op rotations were primarily under Dr. Jonathan Kopechek and was in his Theranostics Ultrasound Laboratory. Her project involved using an ultrasonic flow system for long-term preservation of red blood cells with a collaboration with Dr. Michael Menze in the Biology Department at the University of Louisville. Her focus then shifted to transfection methods and the use of sonoporation as a non-viral transfection method for CAR-T therapy and began the collaboration with Dr. Kavitha Yaddanapudi. Currently, Emily is finishing her Master of Engineering degree in Bioengineering at the University of Louisville under Dr. Jonathan Kopechek and expects to graduate at the beginning of August 2019. She will then be relocating to the Baltimore/Washington DC area to continue her research career as a Biologist I in a respiratory toxicology laboratory under Dr. Holger Behrsing.